

# Parametric renal blood flow imaging using [ $^{15}\text{O}$ ]H $_2\text{O}$ and PET

Nobuyuki Kudomi · Niina Koivuviita ·  
Kaisa E. Liukko · Vesa J. Oikonen · Tuula Tolvanen ·  
Hidehiro Iida · Risto Tertti · Kaj Metsärinne ·  
Patricia Iozzo · Pirjo Nuutila

Received: 14 May 2008 / Accepted: 17 October 2008 / Published online: 3 December 2008  
© Springer-Verlag 2008

## Abstract

**Purpose** The quantitative assessment of renal blood flow (RBF) may help to understand the physiological basis of kidney function and allow an evaluation of pathophysiological events leading to vascular damage, such as renal arterial stenosis and chronic allograft nephropathy. The RBF may be quantified using PET with H $_2^{15}\text{O}$ , although RBF studies that have been performed without theoretical evaluation have assumed the partition coefficient of water ( $p$ , ml/g) to be uniform over the whole region of renal tissue, and/or radioactivity from the vascular space ( $V_A$ , ml/ml) to be negligible. The aim of this study was to develop a method for calculating parametric images of RBF ( $K_1$ ,  $k_2$ ) as well as  $V_A$  without fixing the partition coefficient by the basis function method (BFM).

**Methods** The feasibility was tested in healthy subjects. A simulation study was performed to evaluate error sensitivities for possible error sources.

**Results** The experimental study showed that the quantitative accuracy of the present method was consistent with nonlinear least-squares fitting, i.e.  $K_{1,\text{BFM}}=0.93K_{1,\text{NLF}}-0.11$  ml/min/g ( $r=0.80$ ,  $p<0.001$ ),  $k_{2,\text{BFM}}=0.96k_{2,\text{NLF}}-0.13$  ml/min/g ( $r=0.77$ ,  $p<0.001$ ), and  $V_{A,\text{BFM}}=0.92V_{A,\text{NLF}}-0.00$  ml/ml ( $r=0.97$ ,  $p<0.001$ ). Values of the Akaike information criterion from this fitting were the smallest for all subjects except two. The quality of parametric images obtained was acceptable.

**Conclusion** The simulation study suggested that delay and dispersion time constants should be estimated within an accuracy of 2 s.  $V_A$  and  $p$  cannot be neglected or fixed, and reliable measurement of even relative RBF values requires that  $V_A$  is fitted. This study showed the feasibility of measurement of RBF using PET with H $_2^{15}\text{O}$ .

**Keywords** Positron emission tomography · Renal blood flow · Compartment model · Parametric image

N. Kudomi (✉) · K. E. Liukko · V. J. Oikonen · T. Tolvanen ·  
P. Iozzo · P. Nuutila  
Turku PET Centre, University of Turku,  
P.O. Box 52, FIN-20521 Turku, Finland  
e-mail: nobuyuki.kudomi@tyks.fi

N. Koivuviita · R. Tertti · K. Metsärinne · P. Nuutila  
Department of Medicine, University of Turku,  
Turku, Finland

H. Iida  
Department of Investigative Radiology,  
Advanced Medical-Engineering Center,  
National Cardiovascular Center-Research Institute,  
5-7-1, Fujishirodai,  
Suita, Osaka 565-8565, Japan

P. Iozzo  
Institute of Clinical Physiology, National Research Council,  
56100 Pisa, Italy

## Introduction

The quantitative assessment of renal blood flow (RBF) may help to understand the pathophysiological basis of kidney function and to evaluate pathophysiological events leading to vascular damage, such as renal arterial stenosis and chronic allograft nephropathy. The quantitative estimation of RBF by the use of H $_2^{15}\text{O}$  and dynamic PET has been developed and demonstrated by Nitzsche et al. [1]. The kinetic model of H $_2^{15}\text{O}$  is based on the assumptions that all activity is extracted by the parenchyma, extraction is very rapid, and tubular transport has not started or is insignificant at a level that does not influence the calculation of RBF [1–5]. With these assumptions, RBF has been estimated based on regions of interest (ROI) by the H $_2^{15}\text{O}$

dynamic PET approach [1, 3, 4]. Also, calculations to produce parametric images of RBF has been reported [5]. However, the quantitative computation of RBF has so far assumed that the blood/tissue partition coefficient of water ( $p$ , ml/g) is uniform for the whole region of renal tissue [3, 4], and/or that the contribution of radioactivity from the vascular space is negligible [5–7]. The influence on quantitative accuracy of these assumptions is unknown.

In previous studies RBF has been computed from the uptake rate ( $K_1$ , ml/min/g) [1–7]. Some studies also simultaneously computed the partition coefficient ( $p$ ) [6, 7], and the apparent  $p$  values obtained ranged between 0.52 and 0.78 ml/g. From the published values of water content for tissue (76%) and blood (81%) [8], the  $p$  value can be physiologically determined as:  $p_{\text{phys}}=0.94$  ml/g [9]. The much smaller apparent  $p$  value might be due to the tissue mixture (or a partial volume effect) [10, 11] because of the composite structure of the kidney. The effects of the tissue mixture affect mostly  $K_1$  and not clearance rate ( $k_2$  min<sup>-1</sup>). Therefore the clearance rate of H<sub>2</sub><sup>15</sup>O ( $k_2$  min<sup>-1</sup>) multiplied by  $p_{\text{phys}}$  could be used for the calculation of blood flow rather than  $K_1$  (ml/min/g) [11] when the effect of the tissue mixture is not negligible, although it is unknown how the glomerular filtration rate (GFR) additionally contribute to  $k_2$ . Thus, the influence of GFR on  $k_2$  should be evaluated and allowed for in the computation of RBF.

The aim of this study was to develop a method to simultaneously calculate parametric images of  $K_1$  and  $k_2$  as well as the arterial blood volume ( $V_A$ , ml/ml). The feasibility in terms of quantitative accuracy and image quality of calculated images was experimentally tested in healthy subjects. GFR was measured in each subject to investigate how much it contributes to the clearance rate ( $k_2$ , min<sup>-1</sup>). A simulation study was also performed to evaluate error sensitivities for possible error sources.

## Materials and methods

### Theory

The present formula was characterized by simultaneously estimating multiple parameters of uptake rate constant ( $K_1$ , ml/min/g) and clearance rate constant ( $k_2$  ml/g) as well as activity concentration in the arterial vascular space ( $V_A$ , ml/ml). The kinetic model for H<sub>2</sub><sup>15</sup>O was based on a single-tissue compartment model as follows:

$$Ci(t) = (1 - V_A) \cdot K_1 \cdot A_w(t) \otimes e^{-k_2 t} + V_A \cdot A_w(t) \quad (1)$$

where  $Ci(t)$  (Bq/ml) is radioactivity concentration in a voxel of PET image,  $A_w(t)$  (Bq/ml) is the arterial input function, and  $\otimes$  indicates the convolution integral.

In the present computation, we applied a basis function method (BFM) as introduced by Koeppel et al. [12] to compute the cerebral blood flow parametric image as well as the clearance rate constant simultaneously. Gunn et al. [13] applied this method to parametric imaging of both binding potential and the delivery of ligand relative to the reference region. The computation method has also been applied to myocardial blood flow studies to compute the uptake, clearance rates and blood volume [14, 15]. The BFM procedure for the present RBF computation is illustrated in Fig. 1. The BFM method enables parametric images to be computed by using linear least squares together with a discrete range of basis functions as the parameter value for  $k_2$  incorporating the nonlinearity and covering the expected physiological range. The corresponding basis functions formed are:

$$F(k_2, t) = A_w(t) \otimes e^{-k_2 t} \quad (2)$$

For a physiologically reasonable range of  $k_2$ , i.e.  $0 < k_2 < 15.0$  ml/min/g, 1,500 discrete values for  $k_2$  were found to

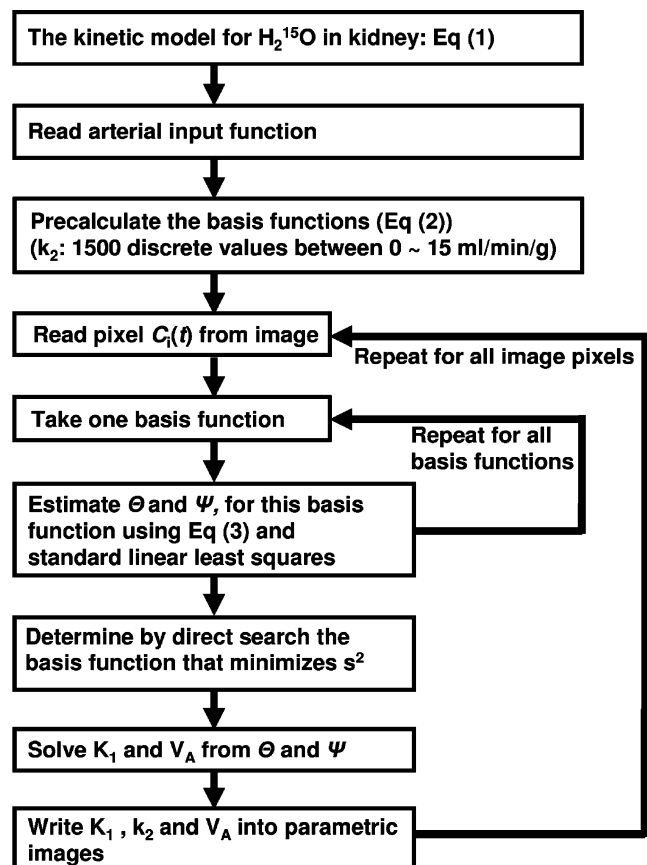


Fig. 1 Schematic diagram of the computation procedure by the BFM

be sufficient. Then Eq. 1 can be transformed for each basis function into a linear equation:

$$\begin{aligned}
 Ci(t) &= \Theta \cdot F(k_2, t) + \Psi \cdot A_w(t) \\
 \Theta &= (1 - V_A) \cdot K_1 \\
 \Psi &= V_A
 \end{aligned}
 \tag{3}$$

Hence for fixed values of  $k_2$ , the remaining two parameters  $\Theta$  and  $\Psi$  can be estimated using the given basis function by standard linear least squares, and are represented as  $\Theta_{k_2}$  and  $\Psi_{k_2}$ . The value  $k_2$  for which the residual sum of squares

$$s(k_2)^2 = \sum_t (Ci(t) - \Theta_{k_2} \cdot F(k_2, t) - \Psi_{k_2} \cdot A_w(t))^2
 \tag{4}$$

is minimized is determined by a direct search, and associated parameter values for this solution ( $K_1$ ,  $k_2$ ,  $V_A$ ) are obtained.

### Subjects

Six healthy human subjects (the demographics are shown in Table 1) were studied under basal conditions and stimulation (after enalapril infusion) conditions. All subjects were nonsmokers and none of them was taking any medication. All subjects gave written informed consent. The study was approved by the Ethics Committee of the Hospital District of South-Western Finland, and was conducted in accordance with the Declaration of Helsinki as revised in 1966.

**Table 1** Baseline characteristics of the six subjects studied

Characteristic	Mean±SD
Age (years)	58±5
Plasma creatinine (μmol/l)	85±10
Estimated GFR (ml/min) <sup>a</sup>	78±4
Weight (kg)	82.8±4.5
Body mass index (kg/m <sup>2</sup> )	26.6±2.2
Blood pressure (mmHg)	
Systolic	136±11
Diastolic	82±4
Heart rate (min <sup>-1</sup> )	57±5
Fasting plasma total cholesterol (mmol/l)	5.3±1.0
Fasting plasma high density cholesterol (mmol/l)	1.5±0.4
Fasting plasma triglycerides (mmol/l)	1.2±0.4
Fasting plasma low density cholesterol (mmol/l)	3.2±0.8
Blood haemoglobin (g/l)	144±12
Fasting plasma glucose (mmol/l)	5.4±0.4

<sup>a</sup> Estimated according to the Modification of Diet in Renal Disease study equation.

### PET experiments

PET was carried out in 2-D mode using a GE Advance scanner (GE Medical Systems, Milwaukee, WI). After a 300-s transmission scan, two scans were undertaken with injection of H<sub>2</sub><sup>15</sup>O (1.0 to 1.5 GBq) into the cephalic vein of the right forearm. The first scan was under resting conditions and the other was under stimulated conditions, namely 20 min after infusion of 0.5 mg enalapril. The scan protocol consisted of 20 frames over a total of 240 s (15×4 s, and 5×10 s). During PET scanning, blood was withdrawn continuously through a catheter inserted into the left radial artery using a peristaltic pump (Scanditronix, Uppsala, Sweden). Radioactivity concentrations in the blood were measured with a BGO coincidence monitor system. The detectors had been cross-calibrated to the PET scanner via an ion chamber [16]. GFR was also measured in each subject [17]. To obtain the PET equivalent flow ratio for GFR, a kidney weight of 300 g and a cortex ratio of 70% were assumed [8].

### Data processing

Dynamic sinogram data were corrected for dead time in each frame in addition to detector normalization. Tomographic images were reconstructed from corrected sinogram data by the OSEM method using a Hann filter with a cut-off frequency of 4.6 mm. Attenuation correction was applied with the transmission data. A reconstructed image consisted 128×128×35 matrix size with a pixel size of 4.3×4.3 mm and 4.2 mm with 20 frames. Measured arterial blood time–activity curves (TAC) were calibrated to the PET scanner and corrected for the dispersion ( $\tau=5$  and 2.5 s for intrinsic and extrinsic, respectively) [18] and delay [19]. The corrected blood TAC was used as the input function.

A set of  $K_1$ ,  $k_2$  and  $V_A$  images was generated according to the BFM formula described above, using a set of dynamic reconstructed images and input function. Computations were programmed in C environment (gcc 3.2) on a Sun workstation (Solaris 10 Sun Fire 280R) with 4 GB of memory and two Sparcv9, 900-MHz CPUs.

### Data analysis

A template ROI obtained by summing whole frames of a reconstructed dynamic image was drawn on an image of the whole region of each kidney (average ROI size for the all subjects was 153±43 cm<sup>3</sup>). Also, a ROI was drawn on a region of high tracer accumulation on the summed image as an assumed cortical region. Functional values of  $K_1$ ,  $k_2$  and  $V_A$  were extracted from both ROIs, i.e. for the whole region and the cortical region, respectively. Data re shown individually or as means±SD. Student’s paired *t* test was

used for comparisons between the physiological states and  $p$  values  $<0.05$  were considered significant.

The ROI for the whole region was divided plane-by-plane into subregions of ten pixels each. The subregions were created by extracting pixels first from the horizontal direction and then from the vertical direction inside the whole ROI in each slice. Each subregion consisted of a single area with the same number of pixels. Functional values of  $K_1$ ,  $k_2$  and  $V_A$  were extracted from each subregion. Tissue TACs were also obtained for each subregion from corresponding dynamic images. The three parameters  $K_1$ ,  $k_2$  and  $V_A$  were estimated using the Eq. 1 and the input function fitted to the tissue TACs by the nonlinear least-squares fitting method (NLF, Gauss-Newton method). Functional values of  $K_1$ ,  $k_2$  and  $V_A$  from corresponding subregions were then compared between the methods. Regression analysis was performed.

The model relevancy introducing  $p$  and/or  $V_A$  into the computation was tested using the Akaike Information Criterion (AIC) [20]. The most appropriate model provides the smallest AIC. The tissue TACs from the subregions were fitted and AICs were computed for models with the three parameters  $K_1$ ,  $k_2$  and  $V_A$ , fixing  $p$  ( $=K_1/k_2$ ) at 0.35 ml/g (mean value obtained in the present subjects), fixing  $V_A$  at 0 ml/ml, and fixing  $V_A$  at 0.15 ml/ml (mean value obtained in the present subjects).

#### Error analysis in the simulation

Error propagation from errors in the input function for the present BFM formula was analysed for two factors: delay and dispersion in arterial TAC. It is known that the measured arterial TAC is delayed and more dispersed relative to the true input TAC in the kidney because of the time for transit of blood through the peripheral artery and the catheter tube before reaching the detector [18, 19]. Calculations of RBF so far have employed a fixed partition coefficient ( $p$ ,  $=K_1/k_2$ , ml/g) and/or assumed the blood volume ( $V_A$ , ml/ml) as negligible throughout the whole renal region and do not estimate it regionally. BFM formulae with a fixed value of  $p$  (BFM-pfix) and blood volume  $V_A$  (BFM-vfix) in addition to the present BFM formula, and the error in these formulae, were analysed.

A typical arterial input function obtained from the present PET study was used in the present simulation as the true input function. Applying this input function to the water kinetic model in Eq. 1, a tissue TAC was created assuming values for normal kidney tissue ( $K_1=2.0$  ml/min/g,  $V_A=0.14$  ml/g [5], and  $p=0.4$  ml/g, corresponding to the estimated means in cortical region in all subjects in this study).

Time in the input function was shifted from  $-4$  to  $4$  s to simulate the error sensitivity due to the error in the time

delay, where a positive error represents an over-correction of the time delay. The input function was convoluted or deconvoluted with a simple exponential [18] by shifting the time constant from  $-4$  to  $4$  s to simulate the error sensitivity due to error in dispersion correction, where a negative error represents under-correction, as described previously [18, 21]. Values of  $K_1$  and  $k_2$  were calculated using simulated input functions and the tissue TACs based on the BFM formula. Errors in these calculated  $K_1$  and  $k_2$  values are presented as percentage differences from the assumed values. Then, the value of  $p$  was varied from 0.3 to 0.5 ml/g and the tissue TAC was generated as above to simulate the error from the value of  $p$  in BFM-pfix formula. Also, the  $V_A$  value was varied from 0.0 to 0.4 ml/ml and the tissue TAC was generated to simulating the error from  $V_A$  in BFM-vfix formula. Then,  $K_1$  and  $k_2$  were calculated using the true input function and the created tissue TACs, assuming  $p=0.4$  ml/g and  $V_A=0.0$  ml/ml in the BFM-pfix and BFM-vfix formulae, respectively. Error in  $K_1$  and  $k_2$  values due to fixing  $p$  is presented as the percentage difference in  $K_1$  and  $k_2$  as a function of  $p$ . Error in  $K_1$  and  $k_2$  values due to neglecting  $V_A$  is presented as the percentage difference in  $K_1$  and  $k_2$  as a function of  $V_A$ . Also,  $K_1$  and  $k_2$  were computed with  $V_A$  fixed at 0.14 ml/ml in the BFM-vfix formula from the set of the tissue TACs, in which  $K_1$  and  $p$  were fixed at 2.0 ml/min/g and 0.4 ml/g, respectively, and  $V_A$  was varied. The percentage difference in  $K_1$  and  $k_2$  between the two conditions, i.e. the initial ( $K_1=2.0$  ml/min/g and  $V_A=0.14$  ml/ml) and changed conditions (presented as  $\Delta K_1$  and  $\Delta k_2$ , respectively) is presented as a function of the percentage difference in the assumed  $V_A$  from 0.14 ml/ml ( $\Delta V$ ) to investigate the extents to which the change in  $K_1$  and  $k_2$  were estimated when  $K_1$  and  $k_2$  were computed in the BFM-vfix formula.

## Results

### Experiments

The relationships of the regional ROI values of  $K_1$ ,  $k_2$  and  $V_A$  between NLF and BFM are shown in Fig. 2. The regression lines obtained were  $K_{1,\text{BFM}}=0.93K_{1,\text{NLF}}-0.11$  ml/min/g ( $r=0.80$ ,  $p<0.001$ ),  $k_{2,\text{BFM}}=0.96k_{2,\text{NLF}}-0.13$  ml/min/g ( $r=0.77$ ,  $p<0.001$ ), and  $V_{A,\text{BFM}}=0.92V_{A,\text{NLF}}-0.00$  ml/ml ( $r=0.97$ ,  $p<0.001$ ), where the subscripts show the methods used for calculating the parametric values; the slopes were not significantly different from unity.

The fitted curve by the present model estimating  $K_1$ ,  $k_2$  and  $V_A$  fitted better than the other two models fixing  $p$  ( $=K_1/k_2$ ) or  $V_A$ . An example of fitted curves is shown in Fig. 3. Also, the AIC values from three parameter fitting were the smallest for all subjects except two values for two

**Fig. 2** Relationships of (a)  $K_1$ , (b)  $k_2$  and (c)  $V_A$  between the ROI-based NLF method and pixel-based BFM. The regression lines were  $K_{1,BFM}=0.93K_{1,NLF}-0.11$  ml/min/g ( $r=0.80$ ,  $p<0.001$ ),  $k_{2,BFM}=0.96k_{2,NLF}-0.13$  ml/min/g ( $r=0.77$ ,  $p<0.001$ ), and  $V_{A,BFM}=0.92V_{A,NLF}-0.00$  ml/ml ( $r=0.97$ ,  $p<0.001$ )

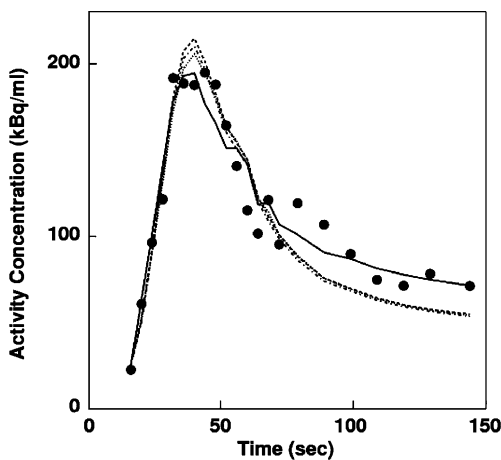
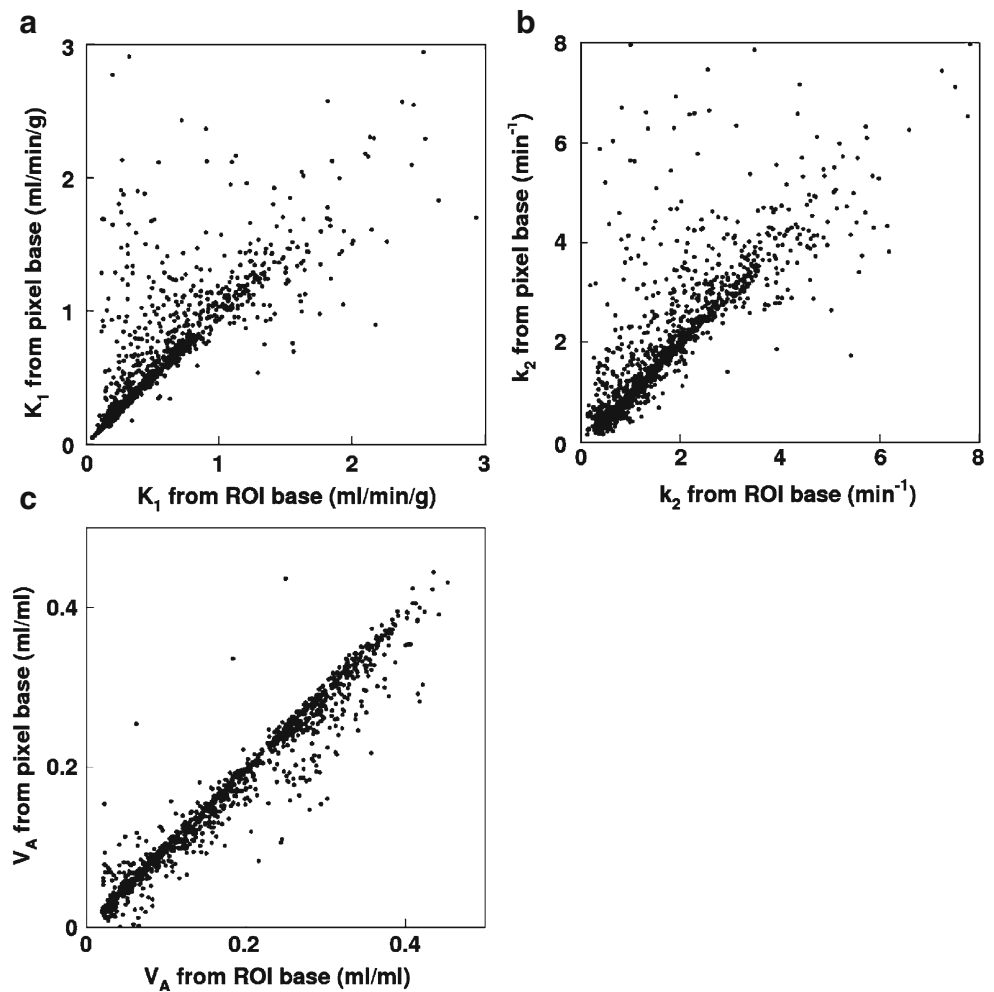


**Fig. 3** Curves fitted to the measured tissue TAC from the different computation methods. Three parameters:  $K_1$ ,  $k_2$  and  $V_A$  were computed.  $p$ -fixed:  $K_1$  and  $V_A$  were computed with  $p$  ( $=K_1/k_2$ ) fixed at 0.35 ml/g.  $V_A$ -fixed:  $K_1$  and  $k_2$  were computed with  $V_A$  fixed at 0.15 ml/g.  $V_A$ -ignored:  $K_1$  and  $k_2$  were computed without taking into account  $V_A$

parameter fitting fixing  $V_A$  in patient 2 and fixing  $p$  in patient 3, although some AIC values were similar (Table 2). These results show that the present method with three parameter fitting is feasible for computing RBF.

Values of  $K_1$ ,  $k_2$ ,  $p_{phys}$  and  $V_A$  were obtained for the whole renal region and cortical region (Table 3). The  $K_1$

**Table 2** AIC values for the models

Subject	Three parameters <sup>a</sup>	$p$ -fixed <sup>b</sup>	$V_A$ -fixed (0.15) <sup>c</sup>	$V_A$ -ignored <sup>d</sup>
1	484±20	519±28	499±15	494±15
2	474±9	486±14	474±9	477±8
3	525±12	523±8.3	527±10	527±7
4	483±14	497±21	501±12	506±13
5	497±18	502±19	508±32	499±13
6	496±11	507±14	500±9	497±9

<sup>a</sup>  $K_1$  and  $k_2$ ,  $V_A$  computed.

<sup>b</sup>  $K_1$  and  $V_A$  computed with  $k_2$  fixing such that  $p=K_1/k_2=0.35$  ml/g.

<sup>c</sup>  $K_1$  and  $k_2$  computed with  $V_A$  fixed at 0.15 ml/g.

<sup>d</sup>  $K_1$  and  $k_2$  computed without taking into account  $V_A$ .

**Table 3** Values of  $K_1$ ,  $k_2 \cdot p_{\text{phys}}$  and  $V_A$  ( $n=6$ ) in the whole renal region and the cortical region calculated by the present method for the baseline conditions and the stimulated conditions

	$K_1$ (ml/min/g)	$k_2 \cdot p_{\text{phys}}$ (ml/min/g)	$V_A$ (ml/ml)	GFR (ml/min/g)
Whole region				
Baseline	1.09±0.33	3.11±1.48	0.15±0.09	0.35±2 <sup>a</sup>
Enalapril-stimulated	1.03±0.44	2.55±1.29	0.16±0.14	
Cortical region				
Baseline	1.57±0.60*	3.64±2.15*	0.18±0.12*	
Enalapril-stimulated	1.42±0.39*	3.55±1.64*	0.25±0.14*	

No significant difference was found between the baseline and stimulated conditions.

\*Difference was significant between the whole and cortical regions.

<sup>a</sup>A kidney weight of 300 g and a cortex ratio of 70% were assumed.

values were smaller than  $k_2 \cdot p_{\text{phys}}$  values and the ratio between them ranged from 0.35 to 0.45, suggesting that  $K_1$  values underestimated RBF due to the partial volume effect. Both  $K_1$  and  $k_2 \cdot p_{\text{phys}}$  were not significantly different between the resting and stimulated conditions for the whole renal region and the cortical region, respectively, although the value of  $V_A$  was higher under the stimulated conditions than under the basal conditions. The GFR obtained was  $78 \pm 4$  ml/min, corresponding to a clearance rate of  $0.37 \pm 0.02$  ml/min/g and to 9.6% of the  $k_2$  obtained for the cortical region under the normal conditions.

Representative  $K_1$  and  $k_2 \cdot p_{\text{phys}}$  images generated by the present method are shown in Fig. 4. The quality of the image is acceptable. The  $K_1$  and  $k_2 \cdot p_{\text{phys}}$  values ranged from 1.5 to 2.0 ml/min/g and 3.0 to 5.0 around cortical region, respectively, and some parts showed higher values than these. The average time required to compute the parametric images was 2 min 23 s.

#### Error analysis

The sizes of the errors introduced in both  $K_1$  and  $k_2$  were less than 20% for estimation of delay and the dispersion

time constant up to 2 s (Fig. 5). The error sensitivity in  $K_1$  and  $k_2$  was 40% when the partition coefficient was 0.35 (Fig. 6). The magnitude of the error was markedly enhanced when the blood volume was ignored (Fig. 7a), and if the arterial blood volume increased by 25%,  $K_1$  and  $k_2$  were overestimated by 20% (Fig. 7a).

#### Discussion

We have presented an approach to generating quantitative  $K_1$ ,  $k_2$  and  $V_A$  images using  $\text{H}_2^{15}\text{O}$  and PET applying the BFM computation method. The validity of this approach in healthy human subjects under resting and stimulated conditions is described. The rate constant values of  $K_1$  and  $k_2 \cdot p_{\text{phys}}$  obtained from the parametric images were consistent against NFL and the quality of the  $K_1$  and  $k_2 \cdot p_{\text{phys}}$  images obtained was acceptable. The smaller  $K_1$  against  $k_2 \cdot p_{\text{phys}}$  values suggested that the  $K_1$  values underestimated the absolute RBF value due to the partial volume effect. The simulation showed that the delay time and dispersion time constant should be estimated within an accuracy of 2 s, and  $V_A$  and  $p$  cannot be ignored/fixed to

**Fig. 4** Representative parametric images of  $K_1$  (left) and  $k_2 \cdot p_{\text{phys}}$  (right) for a subject under baseline conditions. Coronal (upper) and transverse (lower) views are shown

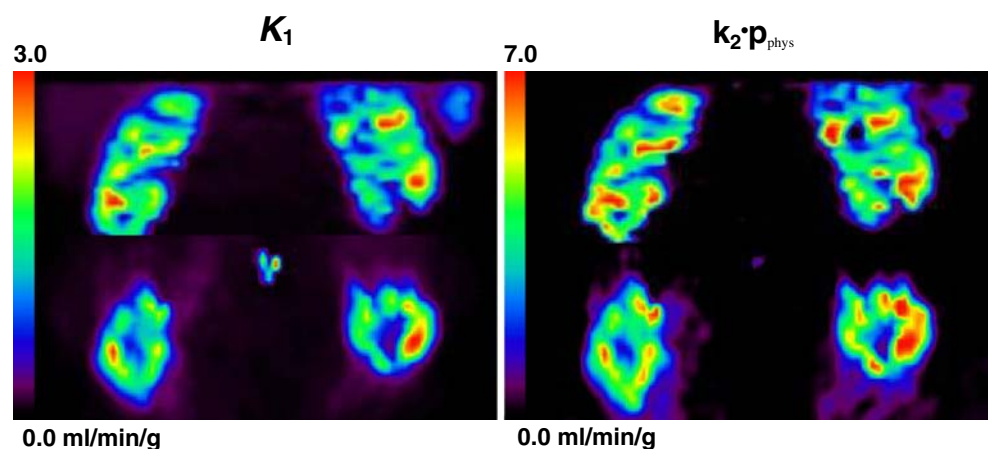
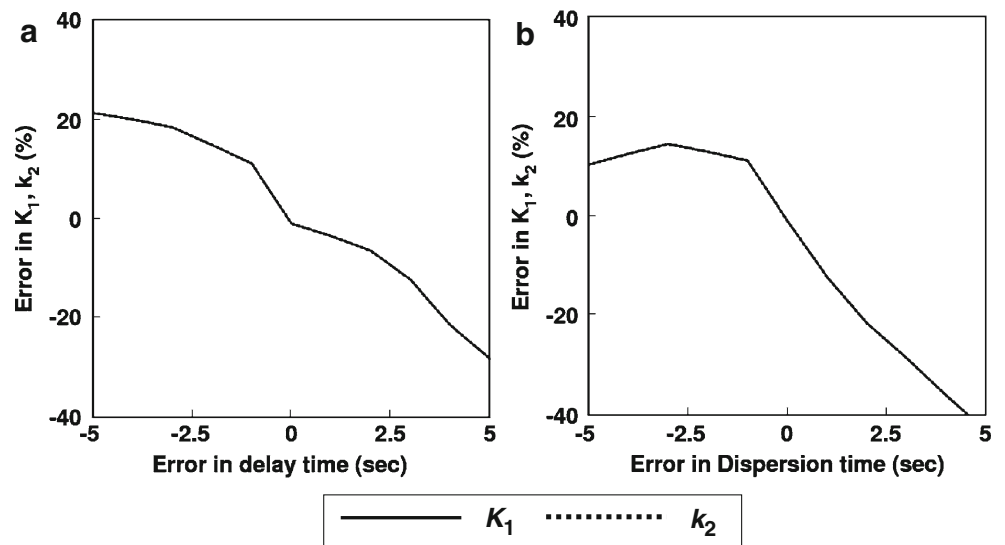


**Fig. 5** Error propagation from the error in input time (a) and dispersion time constant (b) to  $K_1$  and  $k_2$  (the two lines were identical). Positive and negative values of error indicate over- and under-correction of delay time and dispersion time, respectively



estimate the rate constants of  $K_1$  and/or  $k_2$ . Also  $V_A$  cannot be ignored, even when only relative rate constant values are needed. These findings suggest that the present  $k_2$  obtained BFM technique provides an RBF image with reasonable accuracy and quality.

In the present study the rate constants of  $K_1$  and  $k_2$  were experimentally computed, and the ratios obtained ranged from 0.35 to 0.45 ml/g, which corresponds to the apparent kidney–blood partition coefficient. The much smaller apparent  $p$  value might be due to a partial volume effect, as has been demonstrated in a previous brain and cardiac study [10, 11], because of the composite structure of the kidney, the spatial resolution of the reconstructed image and breathing movement of the patient during the scan. When the rate constant  $K_1$  is underestimated due to the partial

volume effect,  $k_2 \cdot p_{\text{phys}}$  could be applied for RBF rather than  $K_1$ . The present study showed that the contribution of GFR to the clearance rate was only 10%, and that  $k_2 \cdot p_{\text{phys}}$  is more appropriate for RBF assessment, although further study of how the GFR changes under stimulated conditions is required. The  $k_2 \cdot p_{\text{phys}}$  value in the cortical region obtained in the present study was  $3.64 \pm 2.15$  ml/min/g under normal condition, a value within the normal range of 4 to 5 ml/min/g reported in the literature [22]. Middlekauff et al. [23–25] applied the ROI base analysis, and showed similar RBF values around 4 ml/min/g. These findings also support the use of  $k_2 \cdot p_{\text{phys}}$  for the calculation of RBF. The different values of RBF between the present study and the previous studies [3–5] might be due to differences in the approaches.

The present computation of RBF by the BFM has two main advantages over the NLF. One is the ability to produce a voxel-by-voxel quantitative parametric map, and the other is faster computing speed. In fact, the parametric images were obtained within a reasonable time, i.e. 2.5 min with an image size of  $128 \times 128$  pixels with 35 slices and 22 frames. The time could be further reduced by applying a threshold to omit pixels with lower values. From a clinical standpoint, voxel-by-voxel analysis is preferred to ROI-based analysis because the operator can independently define ROIs to improve reproducibility, and faster computations are important for analysing very large datasets.

Kinetic parameters estimated by the NLF agreed well with those estimated by the BFM as shown in Fig. 2. The disagreement in some rate constant values between the voxel-based (BFM) and ROI-based computation methods might have been due to the composite structure between the cortical region and its surroundings, or to image noise. Although superior to the NLF in terms of computing speed and ability to generate parametric maps, the BFM shares the same source of errors as the NLF because they use the

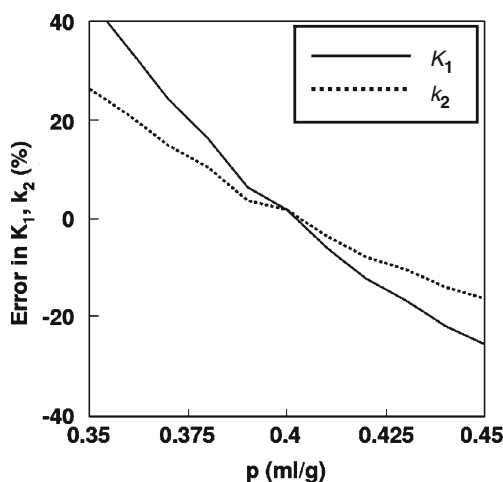
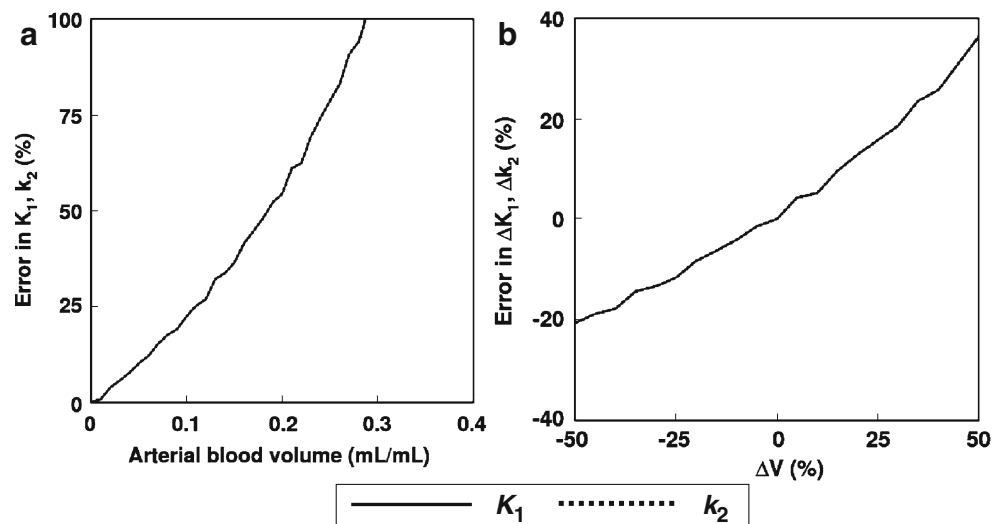


**Fig. 6** Error propagation from the partition coefficient ( $p$ , ml/g) to  $K_1$  and  $k_2$ . When the true  $p$  was varied between 0.6 and 0.8 ml/g, the size of the error in RBF was simulated assuming  $p=0.7$  ml/g

**Fig. 7** **a** Error propagation from the arterial blood volume ( $V_A$ , ml/ml) to  $K_1$  and  $k_2$  (the two lines were identical). When the true  $V_A$  changed from 0.0 to 0.4 ml/ml, the size of the error in  $K_1$  and  $k_2$  calculated assuming  $V_A=0.0$  ml/ml was simulated. **b** Error propagation from the change in arterial blood volume from 0.14 ml/ml ( $\Delta V_A$ ) to the change in  $K_1$  and  $k_2$  from the initial conditions ( $\Delta K_1$  and  $\Delta k_2$ , ml/min/g) (the two lines were identical)



same model and assumption. Delay and dispersion in input function, motion of the patient during a study [26–28], and flow heterogeneity [29] are sources of error for parameters estimated by both the NLF and BFM. Selection of a specific range of  $k_2$  and the number of basis function can affect the accuracy and precision of the estimated parameters in neuroreceptor studies [30, 31]. However, the range was 0 to 15 ml/min/g in the present computation with  $H_2^{15}O$ , and the limits of this range would be acceptable for the present computation. In practice, selection of a wider range and/or a large number of discrete values of the basis function is slow and inefficient against the required accuracy and precision.

The present simulation study showed that if  $V_A$  is neglected or fixed, not only the absolute rate constants, i. e. RBF value, are overestimated, but estimated changes in RBF between two physiological states could be over- or underestimated. These findings suggest that  $V_A$  should be included to obtain either absolute or relative values of RBF. For  $p$ , the present simulation revealed that the error sensitivity in RBF for that value was significant. The values of  $p$  for the whole and cortical regions were 0.35 and 0.42 ml/g, respectively. If the value was fixed at 0.4 ml/g, a 40% overestimation in RBF for regions with a  $p$  of 0.35 occurred. Thus, regional difference in  $p$  introduce error in quantitative RBF values. Also the AIC analysis showed that introducing the extra parameters of  $p$  and  $V_A$  did not increase the AIC value against the others. These findings suggest that both  $p$  and  $V_A$  need to be estimated simultaneously with quantitative RBF, especially when changes under different conditions are assessed.

Knowledge of RBF is mostly needed in determining the severity of renovascular disease. Although the degree of renal artery stenosis is easily diagnosed, its actual effect on RBF remains difficult to quantify. In clinical work,

estimates of GFR have not shown very good accuracy in relation to possible interventional treatment. Also, there is no good clinical method to easily measure single-kidney or regional RBF. We can obtain the effective renal plasma flow (ERPF) by infusing  $p$ -aminohippuric acid and measuring the urine and plasma concentrations, but this method only gives the total ERPF for both kidneys. An alternative is a magnetic resonance (MR) based method, which is problematic in patients with chronic kidney disease, because the contrast agent gadolinium is contraindicated in these subjects [32]. The present PET-related methodology may provide quantitative estimate of regional RBF, and be clinically applicable under conditions such as chronic allograft nephropathy and acute kidney insufficiency. The procedure – as presented here – still involves a small degree of invasiveness because of blood sampling. However, many noninvasive methods for estimating input functions have been proposed [3–5, 23–25, 33, 34], and their implementation will allow RBF to be determined in a fully noninvasive fashion, particularly for clinical purposes.

In conclusion, although some issues remain to be investigated, this study shows the feasibility of measurement of RBF using PET with  $H_2^{15}O$ .

**Acknowledgments** The authors thank the technical staff of the Turku PET Centre for their effort and skill dedicated to this project. This work was supported by the Hospital District of Southwest of Finland and was conducted within the “Centre of Excellence in Molecular Imaging in Cardiovascular and Metabolic Research” supported by the Academy of Finland, University of Turku, Turku University Hospital and Abo Academy. The study was further supported by grants from the Academy of Finland (206359 to P.N.), the Finnish Diabetes Foundation (P.I.), EFSD/Eli-Lilly (P.I.), the Sigrid Juselius Foundation (N.K. and P.I.), and the Novo Nordisk Foundation (P.N.).



## References

- Nitzsche EU, Choi Y, Killion D, Hoh CK, Hawkins RA, Rosenthal JT, et al. Quantification and parametric imaging of renal cortical blood flow in vivo based on Patlak graphical analysis. *Kidney Int* 1993;44:985–96.
- Szabo Z, Xia J, Mathews WB, Brown PR. Future direction of renal positron emission tomography. *Semin Nucl Med* 2006;36:36–50.
- Juillard L, Janier MF, Foucuc D, Lionnet M, Le Bars D, Cinotti L, et al. Renal blood flow measurement by positron emission tomography using  $^{15}\text{O}$ -labeled water. *Kidney Int* 2000;57:2511–18.
- Juillard L, Janier MF, Foucuc D, Cinotti L, Maakel N, Le Bars D, et al. Dynamic renal blood flow measurement by positron emission tomography in patients with CRF. *Am J Kidney Dis* 2002;40:947–54.
- Alpert NM, Rabito CA, Correia DJA, Babich JW, Littman BH, Tompkins RG, et al. Mapping of local renal blood flow with PET and  $\text{H}_2^{15}\text{O}$ . *J Nucl Med* 2002;43:470–75.
- Anderson HL, Yap JT, Miller MP, Robbins A, Jones T, Price PM. Assessment of pharmacodynamic vascular response in a phase I trial of combretastatin A4 phosphate. *J Clin Oncol* 2003;21:2823–30.
- Anderson H, Yap JT, Wells P, Miller MP, Propper D, Price D, et al. Measurement of renal tumour and normal tissue perfusion using positron emission tomography in a phase II clinical trial of razoxane. *Br J Cancer* 2003;89:262–67.
- Snyder WS, Cook MJ, Nasset ES, Karhausen LR, Howells GP, Tipton IH. Report of the Task Group on Reference Man. London: Pergamon Press; 1974. p. 175–77.
- Herscovitch P, Raichle ME. What is the correct value for the brain–blood partition coefficient for water? *J Cereb Blood Flow Metab* 1985;5:65–9.
- Iida H, Law I, Pakkenberg B, Krarup-Hansen A, Eberl S, Holm S, et al. Quantitation of regional cerebral blood flow corrected for partial volume effect using  $\text{O-}^{15}\text{water}$  and PET: I. Theory, error analysis, and stereologic comparison. *J Cereb Blood Flow Metab* 2000;20:1237–51.
- Blomqvist G, Lammertsma AA, Mazoyer B, Wienhard K. Effect of tissue heterogeneity on quantification in positron emission tomography. *Eur J Nucl Med* 1995;22:652–63.
- Koeppel RA, Holden JE, Ip WR. Performance comparison of parameter estimation techniques for the quantitation of local cerebral blood flow by dynamic positron computed tomography. *J Cereb Blood Flow Metab* 1985;5:224–34.
- Gunn RN, Lammertsma AA, Hume SP, Cunningham VJ. Parametric imaging of ligand-receptor binding in PET using a simplified reference region model. *Neuroimage* 1997;6:279–87.
- Watabe H, Jino H, Kawachi N, Teramoto N, Hayashi T, Ohta Y, et al. Parametric imaging of myocardial blood flow with  $^{15}\text{O}$ -water and PET using the basis function method. *J Nucl Med* 2005;46:1219–24.
- Boellaard R, Knaapen P, Rijbroek A, Luurtsema GJ, Lammertsma AA. Evaluation of basis function and linear least squares methods for generating parametric blood flow images using  $^{15}\text{O}$ -water and positron emission tomography. *Mol Imaging Biol* 2005;7:273–85.
- Ruotsalainen U, Raitakari M, Nuutila P, Oikonen V, Sipilä H, Teräs M, et al. Quantitative blood flow measurement of skeletal muscle using oxygen- $^{15}$ -water and PET. *J Nucl Med* 1997;38:314–19.
- Levey A, Bosch J, Lewis J, Greene T, Rogers N, Roth D. A more accurate method to estimate glomerular filtration rate from serum creatinine: a new prediction equation. Modification of Diet in Renal Disease Study Group. *Ann Intern Med* 1999;130:461–70.
- Iida H, Kanno I, Miura S, Murakami M, Takahashi K, Uemura K. Error analysis of a quantitative cerebral blood flow measurement using  $\text{H}_2^{15}\text{O}$  autoradiography and positron emission tomography, with respect to the dispersion of the input function. *J Cereb Blood Flow Metab* 1986;6:536–45.
- Iida H, Higano S, Tomura N, Shishido F, Kanno I, Miura S, et al. Evaluation of regional differences of tracer appearance time in cerebral tissues using  $^{15}\text{O}$  water and dynamic positron emission tomography. *J Cereb Blood Flow Metab* 1988;8:285–88.
- Akaike H. A new look at the statistical model identification. *IEEE Trans Automat Contr* 1974;AC19:716–23.
- Kudomi N, Hayashi T, Teramoto N, Watabe H, Kawachi N, Ohta Y, et al. Rapid quantitative measurement of CMRO $_2$  and CBF by dual administration of  $^{15}\text{O}$ -labeled oxygen and water during a single PET scan – a validation study and error analysis in anesthetized monkeys. *J Cereb Blood Flow Metab* 2005;259:1209–24.
- Ganong WF. Review of medical physiology. 8th ed. Norwalk: Appleton & Lange; 1977. p. 522–45.
- Middlekauff HR, Nitzsche EU, Hamilton MA, Schelbert HR, Fonarow GC, Moriguchi JD, et al. Evidence for preserved cardiopulmonary baroreflex control of renal cortical blood flow in humans with advanced heart failure. *Circulation* 1995;92:395–401.
- Middlekauff HR, Nitzsche EU, Hoh CK, Hamilton MA, Fonarow GC, Hage A, et al. Exaggerated renal vasoconstriction during exercise in heart failure patients. *Circulation* 2000;101:784–89.
- Middlekauff HR, Nitzsche EU, Hoh CK, Hamilton MA, Fonarow GC, Hage A, et al. Exaggerated muscle mechanoreflex control of reflex renal vasoconstriction in heart failure. *J Appl Physiol* 2001;90:1714–19.
- Fulton RR, Meikle SR, Eberl S, Pfeiffer J, Constable CJ. Correction for head movements in positron emission tomography using an optical motion-tracking system. *IEEE Trans Nucl Sci* 2002;49:116–23.
- Bloomfield PM, Spinks TJ, Reed J, Schnorr L, Westrip AM, Livieratos L, et al. The design and implementation of a motion correction scheme for neurological PET. *Phys Med Biol* 2003;48:959–78.
- Woo SK, Watabe H, Choi Y, Kim KM, Park CC, Iida H. Sinogram-based motion correction of PET images using optical motion tracking system and list-mode data acquisition. *IEEE Trans Nucl Sci* 2004;51:782–88.
- Herrero P, Staudenherz A, Walsh JF, Gropler RJ, Bergmann SR. Heterogeneity of myocardial perfusion provides the physiological basis of perfusable tissue index. *J Nucl Med* 1995;36:320–27.
- Cselényi Z, Olsson H, Halldin C, Gulyás B, Farde L. A comparison of recent parametric neuroreceptor mapping approaches based on measurements with the high affinity PET radioligands  $^{11}\text{C}$ FLB 457 and  $^{11}\text{C}$ WAY 100635. *Neuroimage* 2006;32:1690–708.
- Schuitmaker A, van Berckel BN, Kropholler MA, Kloet RW, Jonker C, Scheltens P, et al. Evaluation of methods for generating parametric (R- $^{11}\text{C}$ )PK11195 binding images. *J Cereb Blood Flow Metab* 2007;27:1603–15.
- Martin D, Sharma P, Salman K, Jones RA, Grattan-Smith JD, Mao H, et al. Individual kidney blood flow measured with contrast-enhanced first-pass perfusion MR imaging. *Radiology* 2008;246:241–48.
- Iida H, Kanno I, Takahashi A, Miura S, Murakami M, Takahashi K, et al. Measurement of absolute myocardial blood flow with  $\text{H}_2^{15}\text{O}$  and dynamic positron-emission tomography strategy for quantification in relation to the partial-volume effect. *Circulation* 1988;78:104–15.
- Germano G, Chen BC, Huang S-C, Gambhir SS, Hoffman EJ, Phelps ME. Use of the abdominal aorta for arterial input function determination in the hepatic and renal PET studies. *J Nucl Med* 1992;33:613–20.